From a discrete to a continuum model for static antiphase boundaries

P. Maugis
Institute for Materials Research, McMaster University, Hamilton, Ontario, Canada L8S 4M1
(Received 8 August 1995)

Energetic discrete and continuum models for a heterogeneous ordered alloy of $B2$ structure are presented. In the first instance we use a one-dimensional Ising model in the mean-field approximation where the interaction range is limited to the first-nearest neighbors. From this discrete model the long-range-order parameter and concentration profiles across the (100) nonconservative antiphase boundary (APB) are investigated. The free energy and the interfacial free energy are calculated. The equilibrium equations prove to be coupled via linear gradient terms that contribute to a concentration segregation at the APB, even in a *stoichiometric* compound. The segregation amount is quantified by solving numerically the equilibrium equations, and is shown to be associated with a reduction in the interfacial free energy. The discrete model is extended to two dimensions, from which a continuum approximation is drawn. A three-dimensional generalization that accounts for anisotropic effects is performed. As a particular case, a class of conservative APB's is examined.

I. INTRODUCTION

In their pioneering work Cahn and Hilliard[1] proposed a phenomenological model for a heterogeneous disordered binary alloy in which a quadratic gradient energy term is added to the homogeneous free-energy density, viz.

$$f(c,\vec{\nabla}c)=f^0(c)+\kappa_c(\vec{\nabla}c)^2, \tag{1}$$

where c is the concentration and κ_c is the gradient energy coefficient. This yielded the equilibrium equation

$$\frac{d\Delta f^0}{dc}-2\kappa_c\frac{d^2c}{dx^2}=0. \tag{2}$$

In the dual case of a heterogeneous ordered binary alloy Allen and Cahn[2] have designed the analogous free-energy functional

$$f(\eta,\vec{\nabla}\eta)=f^0(\eta)+\kappa_\eta(\vec{\nabla}\eta)^2, \tag{3}$$

where η is the long-range-order parameter and κ_η is the gradient energy coefficient. This led to the equilibrium equation

$$\frac{d\Delta f^0}{d\eta}-2\kappa_\eta\frac{d^2\eta}{dx^2}=0. \tag{4}$$

Recognizing the necessity of taking into account both η and c parameters when a nonstoichiometric ordered alloy is considered, Krzanowski and Allen[3] proposed the addition of a concentration gradient contribution to Eq. (3), viz.,

$$f(\eta,c,\vec{\nabla}\eta,\vec{\nabla}c)=f^0(\eta,c)+\kappa_\eta(\vec{\nabla}\eta)^2+\kappa_c(\vec{\nabla}c)^2. \tag{5}$$

In doing so they neglected the cross terms in the gradient energy. The resulting two equilibrium equations

$$\frac{\partial\Delta f^0}{\partial\eta}-2\kappa_\eta\frac{d^2\eta}{dx^2}=0 \tag{6}$$

and

$$\frac{\partial\Delta f^0}{\partial c}-2\kappa_c\frac{d^2c}{dx^2}=0 \tag{7}$$

are coupled only through the $\Delta f^0(\eta,c)$ function. The authors showed that these equations account for segregation at the antiphase boundaries (APB's) in a nonstoichiometric alloy. However, their model does not acknowledge segregation in a *stoichiometric* alloy, which is necessary at nonconservative APB's on account of the composition symmetry breaking due to such APB's, as shown in the next paragraph.

Consider a monocrystal of $B2$ structure as consisting of a series of (200) planes occupied alternatively by a majority of A and B atoms (Fig. 1). A particular antiphase domain can be created by ''cutting'' out a slice of the crystal in the middle of two AB pairs of planes and displacing the slice along the $\vec{b}=(1/2)[111]$ vector. The extreme right-hand A plane of the slice is then moved to the vacant sites at the left-hand of the slice. This produces two planar (100) APB's, the left-hand APB defining an excess of A atoms and the right-hand one an excess of B atoms, as indicated below:

$$\cdots ABAB\underline{AA}BABA\cdots BABA\underline{BB}BABAB\cdots.$$

Note that this is an analog of the Gibbs scheme, where a diffuse interface is idealized by an abrupt interface between two homogeneous materials. The excess concentration at each APB clearly breaks the translational symmetry of the composition field. Although the composition field will be smoothed out by relaxation towards equilibrium, the excess concentrations cannot be completely removed unless the APB's themselves are removed. On the contrary, a conservative APB generates no excess concentration in its own plane since in this case the ''cut'' and ''pasted'' plane is of matrix composition. Any comprehensive energetic model will have to account for these various features. It is the motivation of this work to provide such a model.

In this paper a continuum model that incorporates the full coupling effect between concentration and order parameter is

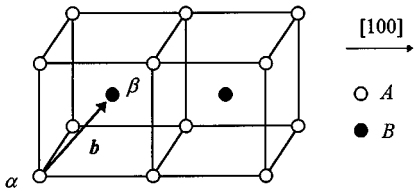

FIG. 1. Atomic structure of a domain in a $B2$-type alloy. The structure consists of the two sublattices α and β translated by the vector $\vec{b}=(1/2)[111]$. Each pair of (200) planes is labeled n.

presented. As a first step, the free-energy function is calculated within the Hillert[4] atomistic framework and the equilibrium equations are established analytically. The consequences of these equations are determined in terms of η and c profiles and interfacial free energy for a planar (100) nonconservative APB. To account for the anisotropy of the $B2$ structure a two-dimensional Ising model is constructed. In the second part of this work the continuum model is presented. Its one- and two-dimensional versions are based upon the continuum approximation of the discrete models. A three-dimensional version is then induced. The consequences of the later on anisotropic segregation are drawn.

II. THE DISCRETE ISING MODEL

Our representation of the sample consists of recognizing two sublattices α and β which in the [100] direction define alternating (200) planes of α and β type, a pair of these planes being indexed by n (Fig. 1). The crystal consists of N biplanes containing Ω atoms each, thus defining a total of $N\Omega$ sites over which atoms A and B are distributed. Two numbers are necessary to define the composition of a given biplane n. We choose the two concentrations c_n^α and c_n^β of B atoms in planes (n,α) and (n,β), or alternatively the local long-range-order parameter

$$\eta_n=\tfrac{1}{2}(c_n^\alpha-c_n^\beta) \tag{8a}$$

and the local average concentration

$$c_n=\tfrac{1}{2}(c_n^\alpha+c_n^\beta). \tag{8b}$$

At this level of approximation we take no account of the short-range order, the state of the whole sample being fully described by the set of parameters $\{\eta_n,c_n\}$. For a closed system the average concentration $\bar{c}$ of the sample is constant and defined by

$$\bar{c}=\frac{1}{N}\sum_{n=1}^{N} c_n=\frac{1}{2N}\sum_{n=1}^{N}\sum_{i=\alpha,\beta} c_n^i. \tag{9}$$

The ordering energy ω for first-nearest-neighbor pair interaction is chosen negative to favor ordering, viz.,

$$\omega=\varepsilon_{AB}-\tfrac{1}{2}(\varepsilon_{AA}+\varepsilon_{BB})<0. \tag{10}$$

In the $B2$ structure the total number of first-nearest neighbors is $Z=8$ and the number of nearest neighbors in an adjacent plane is only $z=(1/2)Z=4$.

A. The mean-field free energy

The free energy per unit site $F=\mathscr{F}/\Omega$, where $\mathscr{F}$ is the total free energy of the sample, is written in terms of the energy of mixing E and the entropy of mixing S, viz.,

$$F=E-TS. \tag{11}$$

The energy of mixing E is calculated by a procedure analogous to that used by Maugis[5] in the fcc structure. The total internal energy is first evaluated as the sum of the interaction energies of each pair of first-nearest neighbors. Each pair involving two sites, a single site contributes to half the interaction energy with each of his neighbors. In the biplane number n, the site (n,α) has z neighbors in the plane $(n-1,\beta)$ and z neighbors in the plane (n,β), while the site (n,β) has z neighbors in the plane (n,α) and z neighbors in the plane $(n+1,\alpha)$. Each pair of sites will contribute according to the probability that it is of BB, AB, or AA type. For example, the pair (n,α)-(n,β) gives the contribution

$$E\begin{pmatrix}\alpha\\ n\end{pmatrix}\begin{pmatrix}\beta\\ n\end{pmatrix}=\frac{1}{2}[c_n^\alpha c_n^\beta\varepsilon_{BB}+(c_n^\alpha c_n'^\beta+c_n'^\alpha c_n^\beta)\varepsilon_{AB}+c_n'^\alpha c_n'^\beta\varepsilon_{AA}]. \tag{12}$$

In Eq. (12) we have used the shorthand notation $c'=1-c$. The contribution of the neighbors of site (n,α) is then

$$E_n^\alpha=zE\begin{pmatrix}\alpha\\ n\end{pmatrix}\begin{pmatrix}\beta\\ n\end{pmatrix}+zE\begin{pmatrix}\alpha\\ n\end{pmatrix}\begin{pmatrix}\beta\\ n-1\end{pmatrix}, \tag{13}$$

while the contribution of the neighbors of site (n,β) is

$$E_n^\beta=zE\begin{pmatrix}\beta\\ n\end{pmatrix}\begin{pmatrix}\alpha\\ n\end{pmatrix}+zE\begin{pmatrix}\beta\\ n\end{pmatrix}\begin{pmatrix}\alpha\\ n+1\end{pmatrix}. \tag{14}$$

The contribution of one lattice cell of plane n is now $E_n=E_n^\alpha+E_n^\beta$, which in full is

$$E_n=\frac{1}{2}\left\{\begin{aligned}&2z[c_n^\alpha c_n^\beta\varepsilon_{BB}+(c_n^\alpha c_n'^\beta+c_n'^\alpha c_n^\beta)\varepsilon_{AB}+c_n'^\alpha c_n'^\beta\varepsilon_{AA}]\\&+z[c_n^\alpha c_{n-1}^\beta\varepsilon_{BB}+(c_n^\alpha c_{n-1}'^\beta+c_n'^\alpha c_{n-1}^\beta)\varepsilon_{AB}+c_n'^\alpha c_{n-1}'^\beta\varepsilon_{AA}]\\&+z[c_n^\beta c_{n+1}^\alpha\varepsilon_{BB}+(c_n^\beta c_{n+1}'^\alpha+c_n'^\beta c_{n+1}^\alpha)\varepsilon_{AB}+c_n'^\beta c_{n+1}'^\alpha\varepsilon_{AA}]\end{aligned}\right\}. \tag{15}$$

The total internal energy of the sample is the sum of the contributions of each of the $(1/2)\Omega$ cells of each biplane n, viz.,

$$\mathscr{E}_{\text{tot}}=\frac{1}{2}\Omega\sum_{n=1}^{N}E_n. \tag{16}$$

The energy of formation equals the difference between the total energy $\mathscr{E}_{\text{tot}}$ and the energy of the separated pure metals $\mathscr{E}_{\text{pure}}$. The latter is

$$\mathscr{E}_{\text{pure}}=\frac{1}{2}N\Omega Z[\bar{c}\varepsilon_{BB}+\bar{c}'\varepsilon_{AA}] \tag{17}$$

which, according to the definition of $\bar{c}$ [Eq. (9)], can be written

$$\mathscr{E}_{\text{pure}}=\frac{1}{2}\Omega Z\left[\frac{1}{2}\varepsilon_{BB}\sum_{n=1}^{N}(c_n^{\alpha}+c_n^{\beta})+\frac{1}{2}\varepsilon_{AA}\times\sum_{n=1}^{N}(c_n'^{\alpha}+c_n'^{\beta})\right]. \tag{18}$$

The energy of formation per unit site is $E=(\mathscr{E}_{\text{tot}}-\mathscr{E}_{\text{pure}})/\Omega$ and is written from Eqs. (16) and (18) as

$$E=\frac{1}{2}\sum_{n=1}^{N}\left[E_n-\frac{1}{2}Z(c_n^{\alpha}+c_n^{\beta})\varepsilon_{BB}-\frac{1}{2}Z(c_n'^{\alpha}+c_n'^{\beta})\varepsilon_{AA}\right]. \tag{19}$$

Incorporating Eq. (15) in (19) yields E as a function of the set of average concentrations $\{c_n^{\alpha},c_n^{\beta}\}$. Some simple algebra shows that the ordering energy ω defined in Eq. (10) can be factorized, leading to

$$E=\frac{1}{2}Z\omega\sum_{n=1}^{N}\left[c_n^{\alpha}+c_n^{\beta}-c_n^{\alpha}c_n^{\beta}-\frac{1}{2}(c_n^{\alpha}c_{n-1}^{\beta}+c_n^{\beta}c_{n+1}^{\alpha})\right]. \tag{20}$$

Grouping the terms into two sums gives the final result

$$E=\frac{1}{2}Z\omega\sum_{n=1}^{N}[c_n^{\alpha}(1-c_n^{\beta})+c_n^{\beta}(1-c_n^{\alpha})]-\frac{1}{2}z\omega\times\sum_{n=1}^{N}[-(c_n^{\alpha}-\tfrac{1}{2})\mathscr{D}c_{n-1}^{\beta}+(c_n^{\beta}-\tfrac{1}{2})\mathscr{D}c_n^{\alpha}]. \tag{21}$$

Here and in the following we use the discrete operators defined by

$$\mathscr{D}\eta_n=\eta_{n+1}-\eta_n, \tag{22a}$$

$$\mathscr{D}^S\eta_n=\tfrac{1}{2}(\eta_{n+1}-\eta_{n-1}), \tag{22b}$$

and

$$\mathscr{D}^2\eta_n=\eta_{n+1}-2\eta_n+\eta_{n-1}. \tag{22c}$$

This anticipates a transformation to continuous derivatives. In the case of a homogeneous alloy, the second sum in Eq. (21) obviously reduces to zero, while the first sum reduces to

$$E=\frac{1}{2}NZ\omega[c^{\alpha}(1-c^{\beta})+c^{\beta}(1-c^{\alpha})]. \tag{23}$$

The second sum in Eq. (21) is then the specific contribution of the heterogeneities of composition in the sample.

We have retained the Hillert[4] approximation of the configurational entropy of mixing which assumes that in each of the sublattices α and β the distribution of A and B atoms is totally random,

$$S=-\frac{1}{2}k\sum_{n=1}^{N}\sum_{i=\alpha,\beta}[c_n^i\ln c_n^i+(1-c_n^i)\ln(1-c_n^i)]. \tag{24}$$

Notice that this form is invariant relatively to any permutation of the c_n^i and therefore does not contribute to the heterogeneity part of the free energy.

Introducing η_n and c_n defined by Eqs. (8a) and (8b) into (21) and (24) we obtain by rearrangement

$$E=Z\omega\sum_{n=1}^{N}[\eta_n^2+c_n(1-c_n)]-\frac{1}{2}z\omega\sum_{n=1}^{N}[(\mathscr{D}\eta_n)^2-(\mathscr{D}c_n)^2+2(c_n-\tfrac{1}{2})\mathscr{D}^S\eta_n-2\eta_n\mathscr{D}^Sc_n] \tag{25}$$

and

$$S=-\frac{1}{2}k\sum_{n=1}^{N}\begin{bmatrix}(c_n+\eta_n)\ln(c_n+\eta_n)+(1-c_n-\eta_n)\ln(1-c_n-\eta_n)\\+(c_n-\eta_n)\ln(c_n-\eta_n)+(1-c_n+\eta_n)\ln(1-c_n+\eta_n)\end{bmatrix}. \tag{26}$$

In (25), $(\mathscr{D}\eta_n)^2$ represents a contribution of the order-parameter heterogeneity, $-(\mathscr{D}c_n)^2$ represents a contribution of the concentration heterogeneity, and the last two cross-terms couple the contributions of order-parameter and concentration heterogeneities. As far as we know, these last two terms have been neglected so far. They are discussed in a following section.

B. The equilibrium equations

We introduce two chemical potentials λ_n and μ_n related, respectively, to η_n and c_n, and show that the equilibrium condition specifies that they both are uniform. The discrete equilibrium equations follow from this requirement.

At equilibrium, $F(\{c_n^i\})$ is extremal with respect to any infinitesimal variation of the parameter set $\{c_n^i\}$ that conserves the overall concentration $\bar{c}$. This leads to the discrete equilibrium equations

$$\partial \Delta F/\partial c_n^\alpha = \partial \Delta F/\partial c_n^\beta = 0, \tag{27}$$

where

$$\Delta F = F - \bar{F} - \mu(c - \bar{c}). \tag{28}$$

$\bar{F}$ is the free energy of the equilibrium homogeneous sample of the same composition $\bar{c}$. μ is a Lagrange multiplier accounting for the conservation of B atoms and can be shown to equate the equilibrium exchange chemical potential (see the Appendix). In order to use the alternate set of parameters $\{\eta_n, c_n\}$ we now introduce the two discrete chemical potentials, $\lambda_n = \partial F/\partial \eta_n$ and $\mu_n = \partial F/\partial c_n$, related, respectively, to the parameters η_n and c_n. Using Eqs. (25) and (26) they are written in full as

$$\lambda_n = -2\omega[-Z\eta_n - \tfrac{1}{2}z(\mathscr{D}^2\eta_n + 2\mathscr{D}^S c_n)] + \frac{1}{2}kT\ln\left(\frac{c_n+\eta_n}{1-c_n-\eta_n} \Big/ \frac{c_n-\eta_n}{1-c_n+\eta_n}\right) \tag{29a}$$

and

$$\mu_n = -2\omega[Z(c_n - \tfrac{1}{2}) + \tfrac{1}{2}z(\mathscr{D}^2 c_n + 2\mathscr{D}^S \eta_n)] + \frac{1}{2}kT\ln\left(\frac{c_n+\eta_n}{1-c_n-\eta_n} \times \frac{c_n-\eta_n}{1-c_n+\eta_n}\right). \tag{29b}$$

The linear relations

$$\lambda_n = \frac{1}{2}\left(\frac{\partial F}{\partial c_n^\alpha} - \frac{\partial F}{\partial c_n^\beta}\right) \tag{30a}$$

and

$$\mu_n = \frac{1}{2}\left(\frac{\partial F}{\partial c_n^\alpha} + \frac{\partial F}{\partial c_n^\beta}\right) \tag{30b}$$

associated with Eq. (28) and (9) allow us to write the equilibrium equations (27) under the form

$$\lambda_n = 0 \quad \text{and} \quad \mu_n = \mu \tag{31}$$

which specifies that the discrete chemical potential λ_n has to be uniformly null and that the discrete chemical potential μ_n has to be uniformly equal to μ. Note that in the particular case when $\bar{c} = 1/2$ we have $\mu = 0$. Incorporating Eqs. (29a) and (29b) into (31) and writing the homogeneous parts in a condensed form yields the discrete equilibrium equations

$$\frac{\partial \Delta F^0}{\partial \eta_n} + z\omega[\mathscr{D}^2\eta_n + 2\mathscr{D}^S c_n] = 0 \tag{32a}$$

and

$$\frac{\partial \Delta F^0}{\partial c_n} - z\omega[\mathscr{D}^2 c_n + 2\mathscr{D}^S \eta_n] = 0, \tag{32b}$$

where ΔF^0 is the homogeneous part of ΔF.

C. The interfacial free energy

We consider the system described in the introduction and consisting of an antiphase domain bounded by two nonconservative (100) planar APB's. The interfacial free energy per unit site of one of these APB's is defined by $\sigma = \Delta F$. Incorporating Eqs. (25) and (26) into (28) and separating the homogeneous and heterogeneous parts into two sums we obtain

$$\sigma = \sum_n \Delta f_n^0 + \sum_n E_n^h, \tag{33}$$

where the heterogeneous part is

$$\sum_n E_n^h = -\frac{1}{2}z\omega\sum_n [(\mathscr{D}\eta_n)^2 - (\mathscr{D}c_n)^2 + 2(c_n - \tfrac{1}{2})\mathscr{D}^S\eta_n - 2\eta_n\mathscr{D}^S c_n]. \tag{34}$$

Using the equilibrium equations (32a) and (32b) and performing the summations in (33) yields

$$\sum_n E_n^h = 0 \tag{35}$$

and the final result

$$\sigma = \sum_n \Delta f_n^0 = -\frac{1}{2}z\omega\sum_n [(\mathscr{D}\eta_n)^2 - (\mathscr{D}c_n)^2]. \tag{36}$$

Notice the negative sign before the concentration contribution in (36). A similar result was found by Gouyet[8] within a mean-field model with repulsive interactions. It is striking that the heterogeneous part of σ reduces to zero. In more details, it appears from the numerical results that the overall positive contribution of the squared differences in ΣE_n^h [first two terms in Eq. (34)] is exactly balanced by the overall negative contribution of the linear differences [last two terms in Eq. (34)], leading to a total null contribution.

D. Numerical results

The equilibrium equations are solved numerically for the system of two APB's described above. Attention is focused on alloys of stoichiometric composition.

In our description of the crystal lattice the pairing of planes is arbitrary. We choose to pair them so as to give rise to biplanes of excess A (B) at the left (right) APB in Gibbs scheme, as indicated below:

$$\cdots AB/AB/\underline{AA}/BA/BA\cdots BA/BA/\underline{BB}/AB/AB\cdots.$$

(type AA) (type BB)

We integrate numerically the kinetic relaxation equations of the $\{c_n^i\}$ derived by Martin[6] to find the equilibrium state that has been proven to identify with the asymptotic limit $t \to \infty$. We have checked that the resulting η_n and c_n profiles are not affected, except by a possible translation along the n axis, by the initial profiles chosen. By adding a random field to the $\{c_n^i\}$ at each step of the integration we make sure not

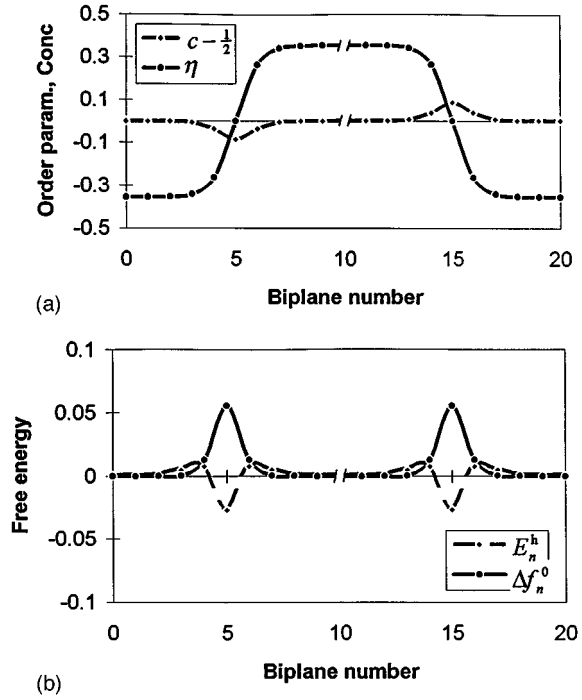

FIG. 2. Two (100) APB's bounding an antiphase domain in a stoichiometric alloy at the temperature of $0.8T_c$. (a) Order parameter and concentration profiles. (b) Homogeneous and heterogeneous parts of the free-energy density.

to reach an unstable or metastable state. Figure 2(a) shows the η_n and c_n profiles computed at the temperature $T=0.8T_c$. As expected, the left (type AA) APB is enriched in A atoms while the right (type BB) APB is enriched in B atoms. The extremum of segregation $|c^m-1/2|$ occurring at the two $\eta=0$ planes is not negligible since it reaches 25% of the equilibrium $\bar{\eta}$ value. The total segregation at one APB is defined by the excess concentration

$$c^{\mathrm{ex}}=\sum_n (c_n-\bar{c}). \tag{37}$$

It is negative for the AA-type APB and positive for the BB-type APB and amounts to 20% of a pure AA or BB biplane (see Table I). By symmetry, the two APB's have opposite segregations such that the total segregation in the sample is zero, as required by the conservation of atoms. The extent of

TABLE I. Results of the numerical calculations. Equilibrium order parameter $\bar{\eta}$, slope $(d\eta/dx)_m$ and width l of the η profile, extremum of segregation $|c^m-1/2|$, total segregation $|c^{\mathrm{ex}}|$, and interface free energy σ for the (100) APB as functions of the reduced temperature T/T_c. Lengths are in units of a and energies are in units of kT_c per unit area $[kT_c=-(1/2)Z\omega]$.

T/T_c	0.6	0.8	0.95
$\bar{\eta}$	0.463	0.355	0.190
$(d\eta/dx)_m$	0.40	0.24	0.0805
l	2.3	2.7	4.7
$\lvert c^m-1/2\rvert$	0.15	0.086	0.022
$\lvert c^{\mathrm{ex}}\rvert$	0.23	0.18	0.095
σ	0.21	0.082	0.011

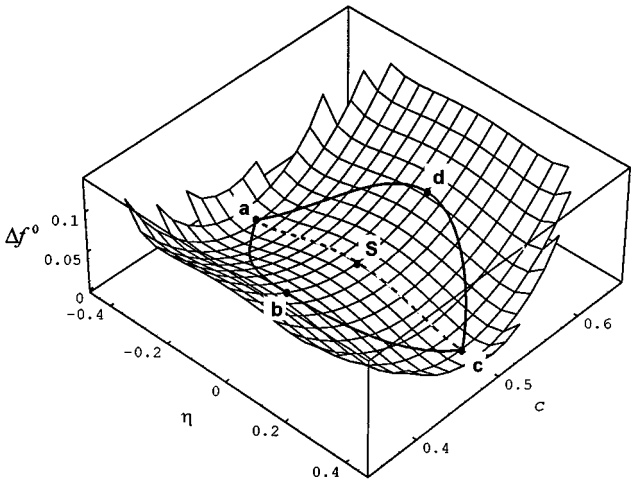

FIG. 3. Path lying on the $\Delta f^0(\eta,c)$ surface corresponding to Fig. 2. As η and c vary across the antiphase domain the path is $abcda$. If c is constrained to 1/2 the path is $aSbSa$. S is the saddle point situated at $\eta=0$ and $c=1/2$.

the segregation profiles is comparable to that of the order-parameter profile as defined by $l=2\bar{\eta}/(d\eta/dx)_{\eta=0}$.

When crossing the antiphase domain, η_n and c_n vary as shown in Fig. 2(a) and accordingly follow a path in the (η,c) plane. In the $(\eta,c,\Delta f^0)$ space this defines a path lying on the $\Delta f^0(\eta,c)$ surface (Fig. 3). We see that if the concentration was constrained to $c=1/2$ the path would pass through the saddle point on the $\Delta f^0(\eta,c)$ surface. Since c actually varies at each APB, the path is a cycle that passes through higher values of Δf^0. As a consequence, the contribution of the homogeneous part of the free energy to the interfacial free energy [Eq. (33)] is slightly higher. However, this increase is largely compensated by the correlative annihilation of the heterogeneous part [Eq. (35)]. In summary, segregation occurs in the disordered region because it provides a decrease in *heterogeneous* free energy that exceeds the correlative increase in homogeneous free energy. Δf_n^0 and E_n^h equilibrium profiles are shown in Fig. 2(b).

Values of interest concerning a single APB are summarized in Table I as functions of temperature T. The extremum of segregation $|c^m-1/2|$ and the total segregation $|c^{\mathrm{ex}}|$ appear to be decreasing functions of temperature, and tend to zero when T approaches the critical temperature of ordering T_c (see Fig. 4).

In nonstoichiometric alloys, APB segregation of the ex-

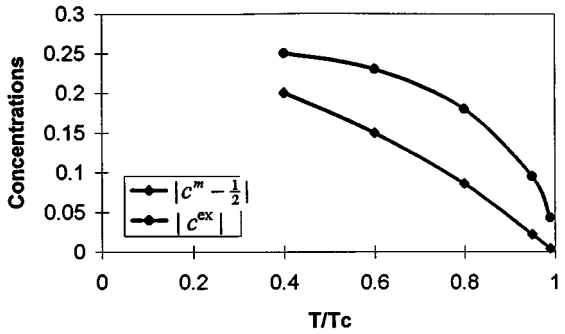

FIG. 4. Extremum segregation and total segregation at the (100) APB in a stoichiometric alloy.

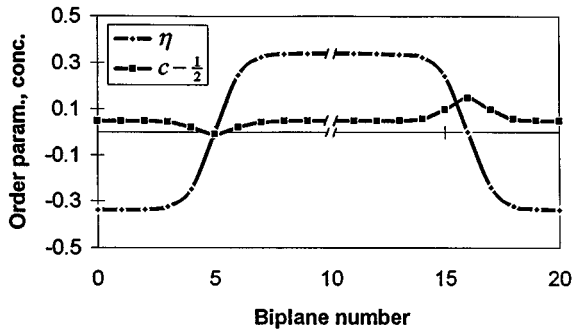

FIG. 5. Order parameter and concentration profiles across an antiphase domain in a nonstoichiometric alloy of average composition $c=0.55$ at the temperature of $0.8T_c$.

cess element is found to be ''superimposed'' with the segregation observed at stoichiometry, leading to a different segregation amount in *AA*- and *BB*-type APB's (see Fig. 5). The details of this matter will be discussed in another paper.

III. THE CONTINUUM MODEL

Numerical simulations show that at temperatures sufficiently close to the critical temperature of ordering the η_n and c_n profiles are smooth. In this range of temperature it is then legitimate to reach a continuum approximation from the discrete equations. For that purpose, the profiles are assumed to be smooth enough so that, to the second order, we can let $n\rightarrow x$ in units of the lattice parameter a and

$$\eta_n \rightarrow \eta(x), \tag{38a}$$

$$(\mathscr{D}\eta_n)^2 \rightarrow (d\eta/dx)^2, \tag{38b}$$

$$\mathscr{D}^S \eta_n \rightarrow d\eta/dx, \tag{38c}$$

$$\mathscr{D}^2 \eta_n \rightarrow d^2\eta/dx^2 \tag{38d}$$

and equivalently for c_n.

A. The continuum free energy

Substituting Eqs. (38) into (25) and (26) and transforming the sums into integrals yields the continuum approximation for the free energy

$$F=\int_{-\infty}^{+\infty} f(\eta,c,\nabla\eta,\nabla c)\,dx \tag{39}$$

with

$$f(\eta,c,\nabla\eta,\nabla c)=f^0(\eta,c)+\kappa\left[\left(\frac{d\eta}{dx}\right)^2-\left(\frac{dc}{dx}\right)^2 +2(c-\tfrac{1}{2})\frac{d\eta}{dx}-2\eta\frac{dc}{dx}\right] \tag{40}$$

and

$$f^0(\eta,c)=Z\omega[\eta^2+c(1-c)]+\frac{1}{2}kT\left[\begin{array}{l}(c+\eta)\ln(c+\eta)+(1-c-\eta)\ln(1-c-\eta)\\ +(c-\eta)\ln(c-\eta)+(1-c+\eta)\ln(1-c+\eta)\end{array}\right]. \tag{41}$$

$f^0(\eta,c)$ is the homogeneous part of the free-energy density $f(\eta,c,\nabla\eta,\nabla c)$ and the gradient energy coefficient in (40) is

$$\kappa=-\tfrac{1}{2}z\omega>0. \tag{42}$$

Only one gradient energy coefficient is necessary to account for the spatial variations of both η and c. This is related to the fact that our model incorporates only one energetic parameter ω, and one lattice parameter a.

In addition to the squared gradients, the heterogeneous part of f includes nonsquared gradients of both η and c [see Eq. (40)]. It shall be noted that the presence of these linear gradient terms does not violate the requirement that f is independent of the orientation of the space. Indeed, consider the change of orientation defined by the transformation $x\rightarrow -x$. η is defined as half the difference in concentration between the left-hand and the right-hand planes of a biplane [Eq. (8a)]. η is then orientation dependent and changes sign when the orientation is reversed. Accordingly, the transformation $x\rightarrow -x$ is accompanied by the transformation $\eta\rightarrow -\eta$ and we can check that these transformations applied to Eq. (40) leave f invariant, as expected.

The last two cross terms in Eq. (40) arise naturally from our lattice model. For the purpose of a qualitative description they could however have been written *a priori*, as shown now. In effect, following Landau and Lifshitz,[7] a quadratic Taylor development of the heterogeneity part of a free energy $f(\eta_1,\eta_2)$ must include linear gradient terms of the form $\eta_i(d\eta_j/dx)$, $i,j=1,2$. The two $\eta_i(d\eta_i/dx)$ terms can be discarded since they are identical to mere gradients and therefore amount to an insignificant constant in the integral of f over space. The two remaining terms can be grouped into their symmetric and their antisymmetric part, respectively,

$$\eta_2(d\eta_1/dx)+\eta_1(d\eta_2/dx) \tag{43}$$

and

$$\eta_2(d\eta_1/dx)-\eta_1(d\eta_2/dx). \tag{44}$$

Equation (43) is a mere gradient and is discarded for the same reason as mentioned above, whereas the remaining term (44) has exactly the form of the cross terms found in our Eq. (40) with the correspondence $\eta_1\rightarrow\eta$ and $\eta_2\rightarrow c-1/2$. We will show in a following section that these often neglected terms are essential to the segregation effect.

We now focus on the two quadratic gradient terms in Eq. (40). Comparing Eq. (40) with the Krzanowski-Allen formula (5) our model identifies $\kappa_\eta=-\kappa_c=\kappa$. It is a remark-

able fact that the gradient energy coefficient κ_c is *negative*. Although it might be argued that this would lead to an instability of the concentration field, the numerical results show that this is not the case, on account of the moderating effect of the remaining cross terms.

B. The equilibrium equations

In this section the equilibrium equations of the system are established, their consequences are drawn in terms of profile characteristics and interfacial free energy, and the results are compared with other authors in the case of a stoichiometric alloy.

Using the definition of κ [Eq. (42)] and applying the set of transformation rules (38) to the discrete equations (32) yields the continuum equilibrium equations

$$\frac{\partial \Delta f^0}{\partial \eta} - 2\kappa\left[\frac{d^2\eta}{dx^2} + 2\frac{dc}{dx}\right] = 0 \tag{45a}$$

and

$$\frac{\partial \Delta f^0}{\partial c} + 2\kappa\left[\frac{d^2 c}{dx^2} + 2\frac{d\eta}{dx}\right] = 0 \tag{45b}$$

with

$$\Delta f^0(\eta,c) = f(\eta,c) - f(\bar{\eta},\bar{c}) - \mu(c-\bar{c}). \tag{46}$$

In Eqs. (45) we have

$$\frac{\partial \Delta f^0}{\partial \eta} = 2Z\omega\eta + \frac{1}{2}kT\,\ln\left(\frac{c+\eta}{1-c-\eta}\Big/\frac{c-\eta}{1-c+\eta}\right) \tag{47a}$$

and

$$\frac{\partial \Delta f^0}{\partial c} = -2Z\omega(c-\tfrac{1}{2}) + \frac{1}{2}kT\,\ln\left(\frac{c+\eta}{1-c-\eta}\times\frac{c-\eta}{1-c+\eta}\right). \tag{47b}$$

Notice that Eqs. (45) are coupled via both the gradient terms and the homogeneity ones. It is easily checked that they are identical to the Euler equations of the continuum free energy [Eqs. (39) and (40)], which are written

$$\frac{\partial \Delta f}{\partial \eta} - \frac{d}{dx}\frac{\partial \Delta f}{\partial(d\eta/dx)} = 0 \tag{48a}$$

and

$$\frac{\partial \Delta f}{\partial c} - \frac{d}{dx}\frac{\partial \Delta f}{\partial(dc/dx)} = 0. \tag{48b}$$

This confirms the self-consistency of the continuum approximation. In two particular cases, when we restrict the description of the alloy to one parameter, the equilibrium equations (45) reduce to classical results. That is, if the concentration is constrained to a constant value throughout the sample, Eqs. (45) reduce to Eq. (4) obtained by Allen and Cahn, with $\kappa_c = -(1/2)z\omega > 0$. In the dual case of a disordered heterogeneous alloy where $\omega > 0$, they reduce by setting $\eta = 0$ to Eq. (2) obtained by Cahn and Hilliard, with $\kappa_\eta = (1/2)z\omega > 0$.

As $\Delta f(\eta, c, \nabla\eta, \nabla c)$ is not an explicit function of x we can write the first integral of the Euler equations (48), viz.,

$$\Delta f - \frac{d\eta}{dx}\frac{\partial \Delta f}{\partial(d\eta/dx)} - \frac{dc}{dx}\frac{\partial \Delta f}{\partial(dc/dx)} = \text{const.} \tag{49}$$

The boundary conditions are the uniform equilibrium state defined by $\eta = \pm\bar{\eta}$, $c = \bar{c}$, and $d\eta/dx = dc/dx = 0$. Under these conditions the constant in Eq. (49) is null. Using expression (40) for f, Eq. (49) gives rise to the equality

$$\Delta f^0(\eta,c) = \kappa\left[\left(\frac{d\eta}{dx}\right)^2 - \left(\frac{dc}{dx}\right)^2\right] \tag{50}$$

verified along the equilibrium profiles. Since $\Delta f^0(\eta,c)$ is always positive, this relation shows that the quadratic gradient terms have an overall positive contribution to the heterogeneity part of the free energy [Eq. (40)]. Applying relation (50) to the point of extremum segregation where $c = c^m$, $\eta = 0$, and $dc/dx = 0$, the slope of the η curve at this point is found to be

$$\left.\frac{d\eta}{dx}\right|_m = \pm\left(\frac{\Delta f^0(0,c^m)}{\kappa}\right)^{1/2}. \tag{51}$$

Since $\Delta f^0(0,c^m)$ is necessarily higher than $\Delta f^0(0,1/2)$ (see Fig. 4), the slope is higher in our case than when the concentration is constrained to $c = 1/2$, leading to a slightly narrower interfacial zone. However, these facts do not lead to a higher interfacial energy, as shown below.

The discrete expression of the interfacial free energy (36) yields, in the continuum case,

$$\sigma = \int_{-\infty}^{+\infty}\Delta f^0(\eta,c)\,dx = \kappa\int_{-\infty}^{+\infty}\left[\left(\frac{d\eta}{dx}\right)^2 - \left(\frac{dc}{dx}\right)^2\right]dx. \tag{52}$$

The second equality of Eq. (52) illustrates clearly how the concentration heterogeneity contributes to a decrease in the interfacial free energy. This result is at variance to that of Krzanowski and Allen [Eq. (1) of Ref. 3] who find a positive contribution of the concentration heterogeneity. In the case of a stoichiometric alloy the first equality in Eqs. (52) can be compared to Allen and Cahn's[2] result $\sigma = 2\int\Delta f^0(\eta,1/2)\,dx$ which is a value about twice as high. So, the relaxation of the concentration field is associated to a reduction of the interfacial free energy by a factor of approximately 2. This shows that segregation at the APB is very favorable energetically.

IV. GENERALIZATION TO HIGHER DIMENSIONALITY

Thus far we have developed a one-dimensional model for planar APB's oriented in the [100] direction. In order to explore other APB orientations a two-dimensional treatment is now undertaken, which will later be generalized to three dimensions. This will allow us to quantify the previous assessment, based upon symmetry arguments, that nonconservative APB's undergo segregation at stoichiometry.

A. The two-dimensional mean-field model

We are concerned with *planar* portions of APB's that include the [001] zone axis. Accordingly, we build a two-dimensional model in the (001) plane. Our representation of the crystal thus consists of N[001] columns containing Ω

cells each. Each column is indexed by the numbers p and q in [001] and [010] directions, respectively. The composition of a given column is defined by the order parameter $\eta_{p,q}=(1/2)(c^{\alpha}_{p,q}-c^{\beta}_{p,q})$ and the concentration $c_{p,q}=(1/2)\times(c^{\alpha}_{p,q}+c^{\beta}_{p,q})$ where $c^{\alpha}_{p,q}$ ($c^{\beta}_{p,q}$) is the average concentration of the α (β) sites contained in the column. Similarly to the one-dimensional case, the configurational entropy of formation is written

$$S=-\frac{1}{2}k\sum_{p,q}\sum_{i=\alpha,\beta}[c^{i}_{p,q}\ln c^{i}_{p,q}+(1-c^{i}_{p,q})\ln(1-c^{i}_{p,q})]. \tag{53}$$

As before, the entropy of formation does not include heterogeneity terms. Following the same steps as for the one dimension case, the energy of formation is found to be

$$E=\frac{1}{2}Z\omega\sum_{p,q}[c^{\alpha}_{p,q}(1-c^{\beta}_{p,q})+c^{\beta}_{p,q}(1-c^{\alpha}_{p,q})] -\frac{1}{2}z\omega\sum_{p,q}\begin{bmatrix} c^{\alpha}_{p,q}(c^{\beta}_{p-1,q}+c^{\beta}_{p,q-1}+c^{\beta}_{p-1,q-1}-3c^{\beta}_{p,q}) \\ +c^{\beta}_{p,q}(c^{\alpha}_{p+1,q}+c^{\alpha}_{p,q+1}+c^{\alpha}_{p+1,q+1}-3c^{\alpha}_{p,q}) \end{bmatrix}. \tag{54}$$

The second sum in Eq. (54) is the specific contribution of the heterogeneities. Introducing the parameters c_{pq} and η_{pq} in Eq. (54) we obtain after some algebra

$$E=Z\omega\sum_{p,q}[\eta^{2}_{p,q}+c_{p,q}(1-c_{p,q})] -\frac{1}{4}z\omega\sum_{p,q}\left\{\begin{array}{l} (\eta_{p+1,q}-\eta_{p,q})^{2}+(\eta_{p,q+1}-\eta_{p,q})^{2}+(\eta_{p+1,q+1}-\eta_{p,q})^{2} \\ -(c_{p+1,q}-c_{p,q})^{2}-(c_{p,q+1}-c_{p,q})^{2}-(c_{p+1,q+1}-c_{p,q})^{2} \\ +(c_{p,q}-\frac{1}{2})[(\eta_{p+1,q}-\eta_{p-1,q})+(\eta_{p,q+1}-\eta_{p,q-1})+(\eta_{p+1,q+1}-\eta_{p-1,q-1})] \\ +\eta_{p,q}[(c_{p+1,q}-c_{p-1,q})+(c_{p,q+1}-c_{p,q-1})+(c_{p+1,q+1}-c_{p-1,q-1})] \end{array}\right\}. \tag{55}$$

Although the homogeneous term of (55) is analogous to that of the one-dimensional model [Eq. (25)], the heterogeneity term is more complicated since it involves finite differences in [100], [010], and [110] directions. To reach a continuum approximation we use the set of transformation rules, valid to the second order,

$$\eta_{p,q}\rightarrow\eta(x,y), \tag{56a}$$

$$(\eta_{p+1,q}-\eta_{p,q})^{2}\rightarrow(\partial\eta/\partial x)^{2}, \tag{56b}$$

$$(\eta_{p,q+1}-\eta_{p,q})^{2}\rightarrow(\partial\eta/\partial y)^{2}, \tag{56c}$$

$$(\eta_{p+1,q+1}-\eta_{p,q})^{2}\rightarrow(\partial\eta/\partial x+\partial\eta/\partial y)^{2}, \tag{56d}$$

$$\eta_{p+1,q}-\eta_{p-1,q}\rightarrow 2\partial\eta/\partial x, \tag{56e}$$

$$\eta_{p,q+1}-\eta_{p,q-1}\rightarrow 2\partial\eta/\partial y, \tag{56f}$$

$$\eta_{p+1,q+1}-\eta_{p-1,q-1}\rightarrow 2(\partial\eta/\partial x+\partial\eta/\partial y), \tag{56g}$$

and equivalently for c. Applying the rules (56) to Eqs. (53) and (55), and transforming the sums into integrals yields the continuum approximation for the free energy

$$F=\iint f(\eta,c,\vec{\nabla}\eta,\vec{\nabla}c)\,dx\,dy \tag{57}$$

with

$$f(\eta,c,\vec{\nabla}\eta,\vec{\nabla}c)=f^{0}(\eta,c)+\kappa\begin{bmatrix} \frac{1}{2}(\vec{\nabla}\eta)^{2}+\frac{1}{2}(\vec{e}\cdot\vec{\nabla}\eta)^{2}-\frac{1}{2}(\vec{\nabla}c)^{2}-\frac{1}{2}(\vec{e}\cdot\vec{\nabla}c)^{2} \\ +2(c-\frac{1}{2})\vec{e}\cdot\vec{\nabla}\eta-2\eta\vec{e}\cdot\vec{\nabla}c \end{bmatrix}, \tag{58}$$

where κ and f^{0} keep their previous definitions [Eqs. (41) and (42)]. In Eq. (58) we have used the two-dimensional vectors $\vec{e}=[11]$ and $\vec{\nabla}=[\partial/\partial x\,\partial/\partial y]$ so that the differential operator $\vec{e}\cdot\vec{\nabla}$ is simply

$$\vec{e}\cdot\vec{\nabla}=(\partial/\partial x+\partial/\partial y). \tag{59}$$

Comparison of Eq. (58) with the one-dimensional version, Eq. (17), illustrates that generalization from one dimension to two dimensions is not straightforward. The simple term-by-term transformation $d/dx\rightarrow\vec{e}\cdot\vec{\nabla}$ is not sufficient and one has to use a particular rule for the square of the gradient, viz.,

$$\left(\frac{d\bullet}{dx}\right)^2 \rightarrow \tfrac{1}{2}[(\vec{\nabla}\bullet)^2+(\vec{e}\cdot\vec{\nabla}\bullet)^2]. \tag{60}$$

This last transformation accounts for the incorporation of the coupling between x and y directions, which is of the form $(\partial\bullet/\partial x)(\partial\bullet/\partial y)$. Notice the absence of the $\vec{\nabla}\eta\cdot\vec{\nabla}c$ term which has been proved nonexistent by the symmetry argument discussed in Sec. III A.

B. The three-dimensional continuum model

The generalization method from two to three dimensions used here consists of inducing the form of the heterogeneous part of the free-energy density f and then deducing the unknown coefficients by comparison with the two-dimensional form [Eq. (58)]. In a Taylor expansion we take into account all terms up to the second degree in η,c and their first spatial derivatives. Accordingly, the general form for f can be written, taking advantage of the cubic symmetry of the crystal,

$$f\left(\eta,c,\left(\frac{\partial\eta}{\partial x_i}\right)_{i=1,3},\left(\frac{\partial c}{\partial x_i}\right)_{i=1,3}\right)=f^0(\eta,c)+\kappa_1\left[(c-\tfrac{1}{2})\left(\sum_i\frac{\partial\eta}{\partial x_i}\right)-\eta\left(\sum_i\frac{\partial c}{\partial x_i}\right)\right]+\kappa_2\left[\sum_i\left(\frac{\partial\eta}{\partial x_i}\right)^2\right]+\kappa_3\left[\sum_{i\neq j}\left(\frac{\partial\eta}{\partial x_i}\right)\left(\frac{\partial\eta}{\partial x_j}\right)\right]$$
$$+\kappa_4\left[\sum_i\left(\frac{\partial c}{\partial x_i}\right)^2\right]+\kappa_5\left[\sum_{i\neq j}\left(\frac{\partial c}{\partial x_i}\right)\left(\frac{\partial c}{\partial x_j}\right)\right]. \tag{61}$$

The term $\Sigma(\partial\eta/\partial x_i)(\partial c/\partial x_j)$ has been discarded since it does not verify the symmetry requirement of invariance by the $(x,y,z,\eta)\rightarrow(-x,-y,-z,-\eta)$ transformation. In the two-dimensional case where $\partial\eta/\partial z=\partial c/\partial z=0$ comparison of Eq. (61) with Eq. (58) identifies the coefficients

$$\tfrac{1}{2}\kappa_1=\kappa_2=\kappa_3=-\kappa_4=-\kappa_5=\kappa. \tag{62}$$

It is easily seen that incorporating (62) into (61) yields exactly the same form for f as in the two-dimensional case [Eq. (58)] provided that the vector $\vec{e}$ is redefined as $\vec{e}=[111]$ instead of $\vec{e}=[11]$. Notice that $\vec{e}$ is now parallel to the vector $\vec{b}=(1/2)[111]$ which defines the translation between the two sites of an atomic cell (see Fig. 1). It is not surprising to find ultimately this vector as part of the free-energy functional since it is intimately related to the definitions of η and c.

We can check that in the particular case of a (100) planar portion of an APB, Eq. (58) with $\vec{e}=[111]$ reduces as expected to the form obtained earlier in this paper. Indeed, substituting $\partial\eta/\partial y=\partial\eta/\partial z=\partial c\partial y=\partial c/\partial z=0$ in Eq. (58) leads directly to the one-dimensional form [Eq. (40)].

The anisotropy effect in the free-energy density [Eq. (58)] is included in the $\vec{e}\cdot\vec{\nabla}$ operator. This vectorial representation allows us to find easily the expression of the free-energy density in the local frame of reference associated to any planar portion of an APB. For this purpose, we define g as the abscissa along the normal $\vec{n}$ to the plane of the APB in the direction of the gradient of η. η and c are now functions of g only. As a result, the differential operator

$$\vec{\nabla}\equiv\vec{n}\frac{d}{dg}. \tag{63}$$

Substituting Eq. (63) in the free-energy density [Eq. (58)] gives

$$f\left(\eta,c,\frac{d\eta}{dg},\frac{dc}{dg}\right)=f^0(\eta,c)+\kappa\left\{\frac{1}{2}[1+(\vec{e}\cdot\vec{n})^2]\times\left[\left(\frac{d\eta}{dg}\right)^2-\left(\frac{dc}{dg}\right)^2\right]+2(\vec{e}\cdot\vec{n})\times\left[(c-\tfrac{1}{2})\frac{d\eta}{dg}-\eta\frac{dc}{dg}\right]\right\}. \tag{64}$$

The scalar product $\vec{e}\cdot\vec{n}$ accounts for the APB orientation dependence. Two particular cases will illustrate this point. In the case of the (100) APB examined in Sec. II, $\vec{n}=[100]$ so that $\vec{e}\cdot\vec{n}=1$ and $g=x$. Substitution into Eq. (64) recovers Eq. (40) of the one-dimensional model, as expected. Consider now the conservative $(1\bar{1}0)$ APB which has the property that the translation vector $\vec{b}$ lies in the plane of the APB. Remembering that $\vec{b}=(1/2)\vec{e}$, the normal vector then verifies $\vec{e}\cdot\vec{n}=0$ and Eq. (64) reduces to the simple form

$$f\left(\eta,c,\frac{d\eta}{dg},\frac{dc}{dg}\right)=f^0(\eta,c)+\frac{1}{2}\kappa\left[\left(\frac{d\eta}{dg}\right)^2-\left(\frac{dc}{dg}\right)^2\right], \tag{65}$$

where the linear gradient terms have disappeared. This equation is similar to that stated by Krzanowski and Allen [Eq. (8) of Ref. 3], except for the sign of κ_η.

Notice that in our description the anisotropy effect is related to the APB orientation *relative to the [111] direction*. This direction is that chosen for the definition of η and c among the eight equivalent directions. The three-dimensional form of the free-energy density is then closely related to the precise definition of the parameters describing the alloy.

Returning to the general case, the three-dimensional Euler equations

$$\frac{\partial\Delta f}{\partial\eta}-\sum_{i=1}^{3}\frac{\partial}{\partial x_i}\frac{\partial\Delta f}{\partial(\partial\eta/\partial x_i)}=0 \tag{66a}$$

and

$$\frac{\partial \Delta f}{\partial c}-\sum_{i=1}^{3}\frac{\partial}{\partial x_i}\frac{\partial \Delta f}{\partial(\partial c/\partial x_i)}=0 \tag{66b}$$

applied to Eq. (58) lead directly to the equilibrium equations

$$\frac{\partial \Delta f^0}{\partial \eta}-2\kappa[\tfrac{1}{2}\vec{\nabla}^2\eta+\tfrac{1}{2}(\vec{e}\cdot\vec{\nabla})^2\eta+2\vec{e}\cdot\vec{\nabla}c]=0 \tag{67a}$$

and

$$\frac{\partial \Delta f^0}{\partial c}+2\kappa[\tfrac{1}{2}\vec{\nabla}^2 c+\tfrac{1}{2}(\vec{e}\cdot\vec{\nabla})^2 c+2\vec{e}\cdot\vec{\nabla}\eta]=0. \tag{67b}$$

In the local frame of reference the equilibrium equations are

$$\frac{\partial \Delta f^0}{\partial \eta}-2\kappa\left\{\frac{1}{2}[1+(\vec{e}\cdot\vec{n})^2]\frac{d^2\eta}{dg^2}+2(\vec{e}\cdot\vec{n})\frac{dc}{dg}\right\}=0 \tag{68a}$$

and

$$\frac{\partial \Delta f^0}{\partial c}+2\kappa\left\{\frac{1}{2}[1+(\vec{e}\cdot\vec{n})^2]\frac{d^2c}{dg^2}+2(\vec{e}\cdot\vec{n})\frac{d\eta}{dg}\right\}=0. \tag{68b}$$

They can be numerically solved for any particular APB, leading to the corresponding $\eta(g)$ and $c(g)$ profiles. It is clear that the terms containing the first spatial derivatives in Eqs. (68) vanish only if the condition $\vec{e}\cdot\vec{n}=0$ is fulfilled. Since these terms are those responsible for the segregation effect at stoichiometry, we conclude that in a stoichiometric alloy all APB's undergo segregation, with various amplitudes, except for the class of conservative APB's that verify $\vec{e}\perp\vec{n}$. The maximum segregation effect is obtained for the (111) APB where $\vec{e}\|\vec{n}$.

The first integral of the Euler equations (68) yields the relation verified along the equilibrium profiles

$$\Delta f^0(\eta,c)=\frac{1}{2}[1+(\vec{e}\cdot\vec{n})]\kappa\left[\left(\frac{d\eta}{dg}\right)^2-\left(\frac{dc}{dg}\right)^2\right], \tag{69}$$

which is the three-dimensional generalization of Eq. (50). The general form of the free-energy density, Eq. (64), allows us to calculate the interfacial free energy for any equilibrium facet of an APB. Taking advantage of Eq. (69) we have

$$\sigma=\int_{-\infty}^{+\infty}\Delta f^0(\eta,c)dg=\frac{1}{2}[1+(\vec{e}\cdot\vec{n})^2]\kappa \times\int_{-\infty}^{+\infty}\left[\left(\frac{d\eta}{dg}\right)^2-\left(\frac{dc}{dg}\right)^2\right]dg. \tag{70}$$

In Eq. (70) the orientation-dependent coefficient

$$\kappa_{\vec{n}}=\frac{1}{2}[1+(\vec{e}\cdot\vec{n})^2]\kappa \tag{71}$$

can be considered as the anisotropic gradient energy coefficient. However it shall be noted that the validity of this simple identification is restricted to Eqs. (70) and (71). The polar plot of $\kappa_{\vec{n}}=(1/2)[1+3\cos^2\theta]\kappa$, where θ is the angle between $\vec{e}$ and $\vec{n}$, exhibits two lobes oriented along the [111] axis, with a sharp neck in the (111) plane. It follows that $\kappa_{\vec{n}}$ reaches its maximum value $\kappa_{\max}=2\kappa$ in the [111] direction and reaches its minimum value $\kappa_{\min}=\kappa/2$ for any APB orientation included in the (111) plane.

V. CONCLUSIONS

We have given an atomistic basis to the continuum free-energy functional for a heterogeneous ordered alloy. The gradient energy coefficients κ_η and κ_c entering the free energy have been related to the parameters of the Ising model. The concentration gradient energy coefficient κ_c proves to be *negative*. Furthermore, the free energy generally contains non-negligible cross terms linear with the gradients. These terms couple the variations of concentration with the variations of order parameter and account for nontrivial segregation behavior. In particular, numerical results show evidence of segregation in a *stoichiometric* alloy at all nonconservative APB's. It is associated to a significant reduction in the interfacial free energy. We believe this effect to be general to all ordered alloys, since it is related to the compositional symmetry breaking of nonconservative APB's.

ACKNOWLEDGMENTS

The author is grateful to Dr. J. S. Kirkaldy for critical comments and revision of an early draft of the manuscript. Part of this work was done at the IMR, McMaster University, Ontario, Canada, under a funding by the Natural Sciences and Engineering Research Council of Canada.

APPENDIX

As can be seen from the definition of $\bar{c}$ in Eq. (9), Eqs. (30) and (31) give the additional equilibrium condition that $\partial\Delta F/\partial\bar{c}=0$. From this the relation between μ and the equilibrium free energy can be derived: $\mu=\partial F/\partial\bar{c}$. We prove in the following that μ is the equilibrium exchange chemical potential $\mu_B-\mu_A$.

Consider an isothermal and isochoric quasistatic transformation during which the composition $\bar{c}$ is changed to $\bar{c}+d\bar{c}$. The total change in free energy in the whole system is

$$d\mathscr{F}=\mu_A dN_A+\mu_B dN_B, \tag{A1}$$

where N_A and N_B are the total number of A and B atoms, respectively. Since the total number of sites is constant, the change of concentration proceeds by exchange of A and B atoms such that $dN_A=-dN_B$ and

$$d\mathscr{F}=(\mu_B-\mu_A)dN_B. \tag{A2}$$

From the definitions $F=\mathscr{F}/\Omega$ and $\bar{c}=N_B/\Omega$ it follows that

$$dF=(\mu_B-\mu_A)d\bar{c}. \tag{A3}$$

Remembering that $\mu=\partial F/\partial\bar{c}$, Eq. (A3) simply shows that $\mu=\mu_B-\mu_A$.

[1] J. W. Cahn and J. E. Hilliard, J. Chem. Phys. **28**, 258 (1958).
[2] S. M. Allen and J. W. Cahn, Acta Met. **27**, 1085 (1979).
[3] J. E. Krzanowski and S. M. Allen, Surf. Sci. **144**, 153 (1984).
[4] M. Hillert, Acta Met. **9**, 525 (1961).
[5] P. Maugis, Ph.D. thesis, Orsay, France, 1994.
[6] G. Martin, Phys. Rev. B **41**, 2279 (1990).
[7] L. D. Landau and E. M. Lifshitz, *Statistical Physics* (Pergamon, New York, 1980), pp. 465–466.
[8] J.-F. Gouyet, Phys. Rev. E **51**, 1695 (1995).